Journal of the European Ceramic Society 42 (2022) 1971–1983

Contents lists available at ScienceDirect

Journal of the European Ceramic Society

journal homepage: www.elsevier.com/locate/jeurceramsoc

Original Article

Liquid metal infiltration of silicon based alloys into porous carbonaceous materials. Part I: Modelling of channel filling and reaction phase formation

Manoj Naikade [a,b,*], Alberto Ortona [c], Thomas Graule [a], Ludger Weber [b]

[a] Empa – Swiss Federal Laboratories for Materials Science and Technology, Dübendorf, Switzerland
[b] Laboratory of Mechanical Metallurgy, Ecole Polytechnique Fédérale de Lausanne, EPFL, Lausanne, Switzerland
[c] Scuola Universitaria Professionale Della Svizzera Italiana, Manno, Switzerland

ARTICLE INFO

Keywords:
LSI
SiC composites
Si-alloy infiltration

ABSTRACT

A relation for an adequate pore fraction needed to obtain residual Si and C free composites via reactive Si-X alloy infiltration is presented. The volume ratio of SiC and carbonaceous phase, the composition of the infiltrating liquid and the apparent density of the preform are used as design entities. The approach allows identifying combinations of these design entities leading to desirable microstructures, e.g. those free of residual silicon or free of excess graphite. The approach gives further access to important post infiltration characteristics like propensity of the various phases.

An idealising mathematical model describing the reactive flow of Si-X alloy in a single micron sized capillary channel of carbon as well as in carbonaceous preforms is presented. The model is further expanded to evaluate the infiltration depth in porous carbonaceous preform for a given composition of Si-X alloy and infiltration temperature. The model is presented for both isothermal and non-isothermal cases.

The analysis is formulated in general terms and is hence applicable to a large variety of Si-C-refractory metal systems of potential interest.

1. Introduction

Liquid silicon infiltration (LSI) into carbonaceous preforms combined with in situ conversion reaction of silicon with carbon to SiC is widely believed to be the most promising and cost-effective route to produce SiC parts [1–4]. In the literature, the LSI process is often advertised as leading to (near) net shape, pore-free SiC material. However, it is often overlooked that the stoichiometric nature of the SiC imposes nearly perfect adequacy between available silicon and available carbon. The former is essentially controlled by the pore volume fraction architectured into the preform and the latter is given by the free carbon concentration per volume in the preform.

A recognised difficulty in such calculations is that the reaction of liquid silicon with the carbonaceous preform material is not volume conservative. This can be seen by looking at the molar volume of liquid silicon at its melting temperature in the 10.8 cm^3 ballpark while SiC has a molar volume of the compound, i.e. for 1 mo of Si and 1 mo of C, 12.5 cm^3 roughly. While there is some latitude in the molar volume of the carbonaceous material, ranging from 3.4 cm^3 for diamond to about 8 cm^3 for glassy carbon, the sum of the molar volumes of liquid Si and the carbonaceous material will always be larger than that of SiC. In an LSI process, in which the liquid silicon is initially brought into the pore space of the preform and then let to react, this will inevitably lead to either porosity after reaction or a global shrinkage of the infiltrated form. In such an event, hoping for "pore-free, net shape material" is optimistic, to say the least. The sometimes used argument that the residual liquid silicon will expand upon solidification and may hence compensate the loss of volume due to the reaction is neglecting the associated disadvantages, i.e. (i) there will be free silicon in the thus formed solid hence limiting the temperature of use to the melting temperature of silicon; (ii) the extent of reaction must be controlled since if there is too much reaction there will be residual porosity and if there is too little reaction the expansion of the liquid silicon upon solidification will initiate cracking of the component.

To justify the hope for a fully dense material without free silicon and without porosity, the LSI process must be conducted such that the reduction in volume due to reaction is constantly compensated by free liquid Si entering the preform. While this view is conceptually appealing, it is based on the, again optimistic, assumption that as reaction proceeds, none of the parts of the preform are separated from the

* Corresponding author at: Empa – Swiss Federal Laboratories for Materials Science and Technology, Dübendorf, Switzerland.
E-mail address: manojknaikade@gmail.com (M. Naikade).

https://doi.org/10.1016/j.jeurceramsoc.2021.12.068
Received 6 September 2021; Received in revised form 23 December 2021; Accepted 24 December 2021
Available online 28 December 2021

external liquid silicon reservoir. In the event that a continuous filling regime can be achieved in LSI, one can predict for what initial preform porosity a fully dense, full SiC body can be achieved. Typical pore volume fractions thus calculated in the literature are in the 55–58 vol.% ballpark for graphite and somewhat below 40 vol.% for glassy carbon. It can be quite challenging to make self-standing handlable performs at that level of porosity based on particles. On the other hand, preforms based on short fibres would be accessible. Another consideration is that full carbonaceous preforms may overheat due to the exothermic nature of the reaction of silicon with carbon to form SiC and therefore lose their integrity due to thermal stresses. Hence, it is a quite often followed path to provide already some SiC particles in the preform to (i) reduce the level of necessary porosity, and (ii) add some thermal mass to the system to keep the temperature variations due to the local reaction small.

Another modification of the LSI process having come lately into focus is the infiltration with silicon alloyed with silicide formers. One of the advantages of the infiltration with liquid silicon alloys is exactly that the fully-fed condition until the end can be somewhat alleviated because the last volume of liquid that is sealed in the pore by clogging of bottle-necks by the reaction is enriched in the alloying element and will eventually convert into a combination of silicides. Some variability in the completeness of the reaction conversion can be compensated by a variability in volume fraction of the silicides in the mixture of silicides that is being formed. Such buffering capacity is also vital in real preforms to compensate for slight variability in the volume fraction of reactive carbonaceous material and porosity on a length scale of the reaction process throughout the preform, i.e. on the level of a few tens of micrometers. The presence of pre-existing SiC and the additional silicide phases render the calculation of adequate starting porosity of the preform more complex.

In all generality, LSI can be conducted by forced infiltration or by spontaneous infiltration. The latter is driven by capillary forces that suck the liquid gradually into the preform while the former can be envisaged by applying pressure on the infiltrating liquid either by a difference in gas pressure inside and outside the preform or by a mechanical pressure applied by a ram as in squeeze casting. Due to the high processing temperatures, the forced infiltration mode is only rarely employed. This is further linked to the fact that for pure silicon infiltration, the only advantage of the forced infiltration would be deeper infiltration since the infiltration time scale is typically short compared to the time scale of clogging of the pore channel system by reaction-formed SiC.

In silicon alloy infiltration another aspect is to be taken into consideration as well: In forced infiltration, the reaction at the interface between liquid and carbonaceous solid is decoupled from the infiltration process. Hence, the liquid will maintain its composition everywhere during the (short) infiltration step and then gradually enrich in the alloying element as silicon is constantly extracted from the liquid by the reaction with the carbonaceous phase of the preform. As the silicon concentration is lowered, the liquidus temperature rises and the residual liquid will eventually transform into solid silicide. For spontaneous infiltration, i.e. infiltration that is driven by capillary forces, the capillary forces will only encourage infiltration when the liquid is wetting the inner walls of the preform. It is well documented that this is only the case when the carbonaceous phases are covered with a thin initial SiC reaction layer that is typically formed at or slightly ahead of the triple line. In such circumstances, the silicon to form the wettable reaction layer comes always from the volume element of liquid right behind the triple line. Naturally, the alloying element becomes enriched at the triple line and may eventually lead to an increase in liquidus temperature that is above the processing temperature of the infiltration. If the enrichment in alloying element cannot be counteracted by diffusion, the infiltration may come prematurely to a halt due to solidification of the (high melting) silicide at the infiltration front. Even if such premature silicide precipitation does not happen, the spontaneous infiltration process will in general lead to an unequal distribution of the silicide forming element, i.e. the silicide forming element will be enriched deeper into the preform and somewhat reduced in the areas close to the ingress surfaces of the infiltrant.

The ramifications of the LSI process both in terms of phases present and conditions for fully dense and fully converted preforms as well as in terms of premature blocking of infiltration by solid silicide phase formation have so far not been discussed in an analytical way in the literature. It is the aim of the present paper to (i) provide general expressions for the adequate preform constitution to obtain fully dense, fully converted SiC/silicide solids in net shape by the LSI process and to (ii) develop an analytical framework to quantitatively predict accessible infiltration depth by spontaneous infiltration of silicon-rich alloys containing silicide formers.

This is the first of three articles series in which we present the analytical models in the part-I, followed by part-II, which shows experimental verification of modelling approaches by infiltration of Si-Zr alloy into idealised microchannels [5], and part-III, which shows experimental verification of conversion products and infiltration depth by infiltration of Si-Zr alloy into carbonaceous and mix SiC/graphite preforms [6].

In Section 2, we present an analytical model to calculate optimal porosity for a carbonaceous C-SiC preform for a given composition of silicide forming Si-X alloy with X being a silicide forming transition metal element like Ti, Zr, Hf, etc., followed by detailed calculations for phases present after reactive infiltration in Section 3.

An analytical model for pore closure due to enrichment of silicide former during reactive flow of Si-X alloy in an idealised rectangular microchannel of carbon is presented in Section 6. The model is further expanded for reactive infiltration of porous carbonaceous C-SiC preform by Si-X alloy in Section 5. A differential model for real life non-isothermal infiltration is proposed in Section 6.

2. Ideal preform porosity to obtain fully dense composites

In the literature, the LSI process is often advertised as leading to (near) net shape, pore-free SiC material. However, it is often overlooked that the stoichiometric nature of the SiC imposes nearly perfect adequacy between available Si and available carbon. The former is essentially controlled by the pore volume fraction architectured into the preform and the latter is given by the free carbon concentration per volume in the preform.

A major difficulty in such calculations is that the reaction of liquid silicon with the carbonaceous preform material is not volume conservative. This can be seen by looking at the molar volume of liquid silicon at its melting temperature in the 10.8 cm^3 ballpark while SiC has a molar volume of the compound, i.e. for 1 mole of Si and 1 mole of C, 12.5 cm^3 roughly. While there is some latitude in the molar volume of the carbonaceous material, ranging from 3.4 cm^3 for diamond to about 8 cm^3 for glassy carbon, the sum of the molar volumes of liquid Si and the carbonaceous material will always be larger than that of SiC. In an LSI process, in which the liquid silicon is initially brought into the pore space of the preform and then let to react, this will inevitably lead to either porosity after reaction or a global shrinkage of the infiltrated form. In such an event, hoping for “pore-free, net shape material” is optimistic, to say the least.

The alternative picture of the LSI process is that the reduction in volume due to reaction is constantly compensated by free liquid Si that enters the preform. While this view is conceptually appealing, it is based on the, again optimistic, assumption that as reaction proceeds, none of the parts of the preform are separated from the external liquid silicon reservoir. The interest of achieving such a processing route would be of course, that the resulting material is indeed pore free. The typical pore volume fractions thus calculated in the literature are in the 55-58 vol.% ballpark for graphite and somewhat below 40 vol.% for glassy carbon [7, 8]. It can be quite challenging to make self-standing handlable performs at that level of porosity based on particles. Furthermore, full carbonaceous preforms may overheat due to the exothermic reaction and lose

their integrity. Hence, it is a quite often followed path to provide already some SiC particles in the preform to (i) reduce the level of necessary porosity, and (ii) add some thermal mass to the system to keep the temperature variations due to the local reaction small.

One of the advantages of the infiltration with liquid silicon alloys is exactly that the fully-fed condition until the end can be somewhat alleviated because the last volume of liquid that is sealed in the pore by clogging of bottle-necks by the reaction is enriched in the alloying element and will eventually convert into a combination of silicides. Some variability in the completeness of the reaction conversion can be compensated by a variability in volume fraction of the silicides in the mixture of silicides that is being formed. Such buffering capacity is also vital in real preforms to compensate for slight variability in the volume fraction of reactive carbonaceous material and porosity on a length scale of the reaction process throughout the preform, i.e. on the level of a few tens of micrometers.

In what follows, the appropriate average pore volume fraction in the preform will be calculated for the ideal case in which liquid silicon alloy is fed continuously until the end of the Si + C conversion reaction. We further aim that there is no residual carbon, no residual porosity and no change in the external dimensions of the preform, i.e. that the whole process is volume conservative. The parameters that will enter the discussion are:

- The volume fraction of silicon carbide particles included in the preform, V_{SiC}.
- The volume fraction of pore space in the preform, V_p.
- The volume fractions of the various sources of carbon in the preform, in the present case graphite, V_{gr}, and pyrolyzed phenolic resin, V_{pc}.
- The molar concentration of silicon in the infiltrating metal, c_{Si}.

We start with the case for infiltration with pure liquid silicon. The goals outlined above will be attained if the sum of the volume fractions occupied by the various forms of carbonaceous material and the pore volume fraction in a preform will correspond to the SiC volume fraction formed by the reaction:

$$V_{\mathrm{gr}} + V_{\mathrm{pc}} + V_p = \left(\frac{V_{\mathrm{gr}}}{V_m^{\mathrm{gr}}} + \frac{V_{\mathrm{pc}}}{V_m^{\mathrm{pc}}}\right) V_m^{\mathrm{SiC}} \tag{1}$$

where $V_m^{\mathrm{gr}}, V_m^{\mathrm{pc}}$, and V_m^{SiC} are the molar volumes of graphite, pyrolysed carbon resulting from pyrolysis of phenolic resin used as binder to make green preforms, and SiC, respectively. Rearranging leads to:

$$V_p = V_{\mathrm{gr}}\left(\frac{V_m^{\mathrm{SiC}}}{V_m^{\mathrm{gr}}} - 1\right) + V_{\mathrm{pc}}\left(\frac{V_m^{\mathrm{SiC}}}{V_m^{\mathrm{pc}}} - 1\right) \tag{2}$$

Now, we consider the case of an alloy with a concentration of $1 - c_{Si}$ in potentially silicide forming species. The silicides are taken to have the general stoichiometry Si_nX. It can easily be seen that the guiding equation formulated above for pure Si will be modified such that the volumes held in the preform by the various forms of carbonaceous materials and pores must not only accommodate the SiC after reaction but also the silicide phase formed. Hence,

$$V_p = V_{\mathrm{gr}}\left(\frac{V_m^{\mathrm{SiC}}}{V_m^{\mathrm{gr}}} - 1\right) + V_{\mathrm{pc}}\left(\frac{V_m^{\mathrm{SiC}}}{V_m^{\mathrm{pc}}} - 1\right) + V_{\mathrm{Si}_nX} \tag{3}$$

In order to be able to determine the volume fractions of the silicides we have to observe that the number of moles of silicon per volume of preform going into reaction-formed SiC, $C_{Si,SiC}$, is

$$\left(\frac{V_{\mathrm{gr}}}{V_m^{\mathrm{gr}}} + \frac{V_{\mathrm{pc}}}{V_m^{\mathrm{pc}}}\right) = C_{\mathrm{Si,SiC}} \tag{4}$$

To this adds the number of moles of silicon per volume entering into the silicide, $C_{\mathrm{Si,Si}_nX}$, whence the amount of alloying element X per volume available for the formation of silicide, C_{X,Si_nX}, is found as

$$C_{X,\mathrm{Si}_nX} = \frac{1 - c_{\mathrm{Si}}}{c_{\mathrm{Si}}}\left(C_{\mathrm{Si,SiC}} + C_{\mathrm{Si,Si}_nX}\right) \tag{5}$$

The number of moles per volume of the preform of element X and the number of moles of silicon entering into the silicide are of course linked by the stoichiometry as

$$C_{\mathrm{Si,Si}_nX} = \mathrm{n}C_{X,\mathrm{Si}_nX} \tag{6}$$

Inserting and rearranging leads to

$$C_{X,\mathrm{Si}_nX} = \frac{\frac{1-c_{\mathrm{Si}}}{c_{\mathrm{Si}}} C_{\mathrm{Si,SiC}}}{\left(1 - \frac{n(1-c_{\mathrm{Si}})}{c_{\mathrm{Si}}}\right)} \tag{7}$$

The volume fraction of silicide at the end of the reaction is then found as

$$V_{\mathrm{Si}_nX} = C_{X,\mathrm{Si}_nX} V_m^{\mathrm{Si}_nX} = \frac{\frac{1-c_{\mathrm{Si}}}{c_{\mathrm{Si}}} C_{\mathrm{Si,SiC}}}{\left(1 - \frac{n(1-c_{\mathrm{Si}})}{c_{\mathrm{Si}}}\right)} V_m^{\mathrm{Si}_nX} = \frac{\frac{1-c_{\mathrm{Si}}}{c_{\mathrm{Si}}}\left(\frac{V_{\mathrm{gr}}}{V_m^{\mathrm{gr}}} + \frac{V_{\mathrm{pc}}}{V_m^{\mathrm{pc}}}\right)}{\left(\frac{(n+1)c_{\mathrm{Si}} - n}{c_{\mathrm{Si}}}\right)} V_m^{\mathrm{Si}_nX} \tag{8}$$

We can insert this expression in the above expression for V_p, yielding:

$$V_p = V_{\mathrm{gr}}\left(\frac{V_m^{\mathrm{SiC}}}{V_m^{\mathrm{gr}}} - 1\right) + V_{\mathrm{pc}}\left(\frac{V_m^{\mathrm{SiC}}}{V_m^{\mathrm{pc}}} - 1\right) + \frac{\frac{1-c_{\mathrm{Si}}}{c_{\mathrm{Si}}}\left(\frac{V_{\mathrm{gr}}}{V_m^{\mathrm{gr}}} + \frac{V_{\mathrm{pc}}}{V_m^{\mathrm{pc}}}\right)}{\left(\frac{(n+1)c_{\mathrm{Si}} - n}{c_{\mathrm{Si}}}\right)} V_m^{\mathrm{Si}_nX} \tag{9}$$

Dividing on both sides by V_p leads to an explicit equation involving the ratios of V_{gr}/V_p and V_{pc}/V_p that must be obeyed:

$$1 = \frac{V_{\mathrm{gr}}}{V_p}\left(\frac{V_m^{\mathrm{SiC}}}{V_m^{\mathrm{gr}}} - 1\right) + \frac{V_{\mathrm{pc}}}{V_p}\left(\frac{V_m^{\mathrm{SiC}}}{V_m^{\mathrm{pc}}} - 1\right) + \frac{\frac{1-c_{\mathrm{Si}}}{c_{\mathrm{Si}}}\left(\frac{V_{\mathrm{gr}}}{V_p}\frac{1}{V_m^{\mathrm{gr}}} + \frac{V_{\mathrm{pc}}}{V_p}\frac{1}{V_m^{\mathrm{pc}}}\right)}{\left(\frac{(n+1)c_{\mathrm{Si}} - n}{c_{\mathrm{Si}}}\right)} V_m^{\mathrm{Si}_nX} \tag{10}$$

We note that the volume fraction of SiC already present in the preform has no effect on the result, as expected. It is just an additional volume that does not intervene in the conversion. The typical preform fabrication process consists in mixing the solid (or liquid) constituents of the preform in certain mass ratios and the pore volume fraction will be a result of the compaction process of the constituents and the decomposition of the polymeric constituent. These mass ratios of the constituents can be converted into volume fraction ratios in the solid phase of the preform:

$$\frac{M_{\mathrm{SiC}}}{m_{\mathrm{SiC}}} V_m^{\mathrm{SiC}} : \frac{M_{\mathrm{gr}}}{m_{\mathrm{gr}}} V_m^{\mathrm{gr}} : \frac{M_{\mathrm{pc}}}{m_{\mathrm{pc}}} V_m^{\mathrm{pc}} = \frac{M_{\mathrm{SiC}}}{\rho_{\mathrm{SiC}}} : \frac{M_{\mathrm{gr}}}{\rho_{\mathrm{gr}}} : \frac{M_{\mathrm{pc}}}{\rho_{\mathrm{pc}}} = V_{\mathrm{SiC}} : V_{\mathrm{gr}} : V_{\mathrm{pc}} \tag{11}$$

We can thus express the volume fraction of carbonaceous material in terms of the volume fraction of graphite as:

$$V_{\mathrm{pc}} = \frac{M_{\mathrm{pc}} \rho_{\mathrm{gr}}}{M_{\mathrm{gr}} \rho_{\mathrm{pc}}} V_{\mathrm{gr}} \tag{12}$$

and, obviously,

$$\frac{V_{\mathrm{pc}}}{V_p} = \frac{M_{\mathrm{pc}} \rho_{\mathrm{gr}}}{M_{\mathrm{gr}} \rho_{\mathrm{pc}}} \frac{V_{\mathrm{gr}}}{V_p} \tag{13}$$

Inserting this into Eq. (10), we find for the ratio of graphite volume fraction and pore volume fraction:

$$1 = \frac{V_{gr}}{V_p}\left(\left(\left(\frac{V_m^{SiC}}{V_m^{gr}} - 1\right) + \frac{M_{pc}\rho_{gr}}{M_{gr}\rho_{pc}}\left(\frac{V_m^{SiC}}{V_m^{pc}} - 1\right)\right) + \frac{\frac{1-c_{Si}}{c_{Si}}\left(\frac{1}{V_m^{gr}} + \frac{M_{pc}\rho_{gr}}{M_{gr}\rho_{pc}}\frac{1}{V_m^{pc}}\right)}{\left(\frac{(n+1)c_{Si}-n}{c_{Si}}\right)} V_m^{Si_nX}\right) \quad (14)$$

Solving for V_{gr}/V_p, leads to

$$\frac{V_{gr}}{V_p} = \frac{1}{\left(\left(\frac{V_m^{SiC}}{V_m^{gr}} - 1\right) + \frac{M_{pc}\rho_{gr}}{M_{gr}\rho_{pc}}\left(\frac{V_m^{SiC}}{V_m^{pc}} - 1\right) + \frac{\frac{1-c_{Si}}{c_{Si}}\left(\frac{1}{V_m^{gr}} + \frac{M_{pc}\rho_{gr}}{M_{gr}\rho_{pc}}\frac{1}{V_m^{pc}}\right)}{\left(\frac{(n+1)c_{Si}-n}{c_{Si}}\right)} V_m^{Si_nX}\right)} = A \quad (15)$$

Of course, the sum of the volume fractions of all elements forming the preform, i.e. SiC, graphite, pyrolyzed phenolic resin, and pores, must equal to 1:

$$V_p + V_{SiC} + V_{gr} + V_{pc} = 1 \quad (16)$$

Rearranging and expressing the volume fraction of SiC and pyrolyzed phenolic resin in the preform by the volume fraction of graphite leads to:

$$\frac{V_{gr}}{V_p}\underbrace{\left(1 + \frac{M_{SiC}\rho_{gr}}{M_{gr}\rho_{SiC}} + \frac{M_{pc}\rho_{gr}}{M_{gr}\rho_{pc}}\right)}_{B} = \frac{(1-V_p)}{V_p} \quad (17)$$

We hence find that the pore volume fraction that leads to complete conversion and no volume change in LSI can be written as

$$AB = \frac{(1-V_p)}{V_p} \quad (18)$$

whence:

$$V_p = \frac{1}{(1+AB)} \quad (19)$$

While the formalism can be applied to any sort of Si-X alloy with X a silicide former, we would like to concentrate on the Si-X system used in our experimental work [5,6], i.e. Si-Zr, in order to be able to get some numerical values. The silicides in this system are of stoichiometry Si_2Zr and SiZr, i.e. the calculations are to be done for $n = 2$ and $n = 1$.

We can now calculate the adequate porosity for a given composition of the preform in terms of the mass ratio of the constituents and see how this value evolves for the liquid metal composition c_{Si} as well as the type of silicide formed. We do this here as an example for a preform based on 70 g of SiC, 20 g of graphite and 6 g of carbon coming from the pyrolysis of 10 g of phenolic resin. The resulting ideal pore volume fraction as a function of the composition of the infiltrant are shown for the silicides Si_2Zr and SiZr in Fig. 1.

The calculated results as seen in Fig. 1 stand by and large to reason: as the potential for silicide formation is increased the larger the pore space for infiltration gets. The more Si can be captured by a given silicide the more additional pore space can be admitted. This is the reason why the line for SiZr passes below the line of Si_2Zr.

The curves indicative for the formation of the silicides (shown in Fig. 1) subdivide the parameter space of pore volume fraction and infiltrant composition in three distinct regions: (i) above the blue curve, there will be free silicon available, even if all carbon is converted; (ii) in the space below the red curve there will most likely be free carbon around even when the reaction is finished; and (iii) between the red and the blue curve there is the "sweet spot" of processing, i.e. the $c_{Zr} - V_p$ combination space that allows a material after the reaction has ended

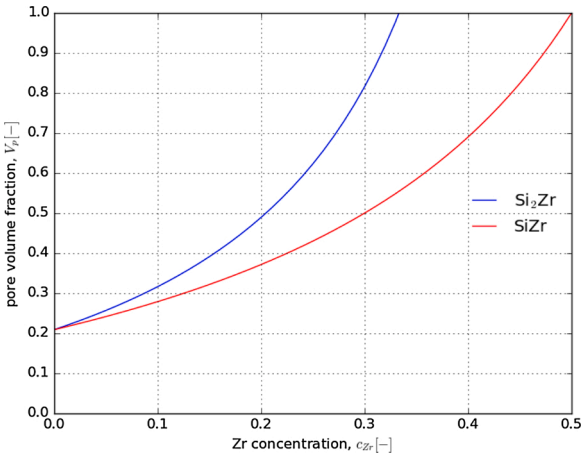

Fig. 1. Evolution of the ideal pore volume fraction with infiltrant concentration in silicide forming element, in the case shown for a preform made of 70 g SiC powder, 20 g graphite and initially 10 g of phenolic resin that after pyrolysis results in 6 g of amorphous carbon. (For interpretation of the references to colour in this figure citation, the reader is referred to the web version of this article.)

that has potentially no pores, and where only SiC and silicides are present. The red line is, however, not a hard limit: if the silicide former is at the same time also a strong carbide former, some of the free carbon can also be bonded in carbides of the infiltrant's alloying element. This, however, depends significantly on the relative stability of the silicides, the X-carbide and SiC. Of course, if ternary phases are present, those may affect the result as well. It is, however, quite common that SiC is stable with the first two stable silicides in many Si-X systems. The "sweet spot" calculation may hence also be applicable to other Si-X systems used in LSI, provided that the adequate values for the molar volumes of the silicides are used.

A last remark is concerned with Si-X systems forming silicides of stoichiometries that cannot be written with integer values for n. In the derivation, there is no need that the n be an integer. For a Mo_5Si_3 silicide, one could well take $n = 0.6$ but would need to calculate the molar volume of Mo_5Si_3 for one mole of Mo-atoms to stay consistent.

3. Detailed calculation of the phases present

As we mentioned above, the curves indicative for the formation of the silicides subdivide the parameter space: pore volume fraction vs. infiltrant composition in three distinct regions: above the blue curve there will be free silicon at the end of the reaction, in the space below the red curve residual free carbon is expected and between the lines there will be a mixture of silicides present.

In order to assess the success of an infiltration apparent density is a common tool to qualify the composite. It is hence important to have an idea about the expected density in the event that the resulting material consists not only of SiC but also of silicides. We formulate in what follows a general approach how the volume fractions of the phases present after full conversion and the resulting density can be estimated. We first consider the space above the blue curve the pore space is larger than would be needed to fully convert the carbonaceous phases into SiC and hence we have to be concerned with the formation of SiC, Si, and the first stable silicide of stoichiometry Si_nX.

We start with a preform that is composed of volume fractions of SiC, graphite, pyrolysed carbon, and pores in volume fractions of V_{SiC}, V_{gr}, V_{pc}, and V_p. We consider the case where the carbonaceous phases will get fully converted, and the resulting composite has the same volume as the apparent volume of the preform. The liquid is supposed to have access to the pore space everywhere until the end of the reaction. The small shrinkage of the liquid corresponding to the composition of the silicide is

neglected. Furthermore, the partial molar volumes of silicon and the silicide former, X, are considered identical and hence the molar volume of the liquid alloy is independent of composition. We look at a volume of the preform of unity such that volume and volume fraction can be used interchangeably. The volume fractions of the phases constituting the unreacted preform can be found based on their mass fractions in the solid and the pore volume fraction, V_p, that can be either measured by, e. g. mercury porosimetry, or inferred from the apparent density of the preform. The relevant relations are:

$$V_p = \left(1 - \frac{\rho_{\text{app}}}{\frac{M_{\text{SiC}}+M_{\text{gr}}+M_{\text{pc}}}{\frac{M_{\text{SiC}}}{\rho_{\text{SiC}}}+\frac{M_{\text{gr}}}{\rho_{\text{gr}}}+\frac{M_{\text{pc}}}{\rho_{\text{pc}}}}}\right) \tag{20}$$

$$V_{\text{SiC}} = \frac{\frac{M_{\text{SiC}}}{\rho_{\text{SiC}}}\rho_{\text{app}}}{M_{\text{SiC}}+M_{\text{gr}}+M_{\text{pc}}} \tag{21}$$

$$V_{\text{gr}} = \frac{\frac{M_{\text{gr}}}{\rho_{\text{gr}}}\rho_{\text{app}}}{M_{\text{SiC}}+M_{\text{gr}}+M_{\text{pc}}} \tag{22}$$

$$V_{\text{pc}} = \frac{\frac{M_{\text{pc}}}{\rho_{\text{pc}}}\rho_{\text{app}}}{M_{\text{SiC}}+M_{\text{gr}}+M_{\text{pc}}} \tag{23}$$

In such circumstances, we can compare the situation in the beginning with volume fractions V_{SiC}, V_{gr}, V_{pc}, and V_p, with that in the end with V_{SiC}, $V_{SiC,react}$, $V_{\text{Si}_n X}$, and $V_{Si,free}$. It must hold:

$$V_p + V_{\text{gr}} + V_{\text{pc}} = V_{\text{SiC,react}} + V_{\text{Si}_n X} + V_{\text{Si,free}} \tag{24}$$

The reacted volume fraction of SiC must be linked to the volume fractions of the carbonaceous phases by:

$$V_{\text{SiC,react}} = \left(\frac{V_{\text{gr}}}{V_m^{\text{gr}}} + \frac{V_{\text{pc}}}{V_m^{\text{pc}}}\right) V_m^{\text{SiC}} \tag{25}$$

For the volume fraction of the first silicide, $V_{\text{Si}_n X}$, we can write with the number of mol of the silicide former, N_X,

$$V_{\text{Si}_n X} = N_X V_m^{\text{Si}_n X} \tag{26}$$

The total number of mol per volume of Si, N_{Si}, having entered the preform by infiltration is linked to N_X by

$$N_{\text{Si}} = N_X \frac{c_{\text{Si}}}{(1-c_{\text{Si}})} \tag{27}$$

Of these, the number of mol per volume, $N_{\text{Si,Si}_n X}$, entering eventually in the solid silicide is

$$N_{\text{Si,Si}_n X} = \text{n}N_X \tag{28}$$

On the other hand, those entering in carbide formation, $N_{Si,SiC\,react}$, is given by

$$N_{\text{Si,SiCreact}} = \left(\frac{V_{\text{gr}}}{V_m^{\text{gr}}} + \frac{V_{\text{pc}}}{V_m^{\text{pc}}}\right) = N_{\text{Si}} - N_{\text{Si,Si}_n X} - N_{\text{Si,free}} = N_X\left(\frac{c_{\text{Si}}}{(1-c_{\text{Si}})} - n\right) - N_{\text{Si,free}} \tag{29}$$

From the starting equation we find

$$V_{\text{Si}_n X} + V_{\text{Si,free}} = V_p + V_{\text{gr}} + V_{\text{pc}} - V_{\text{SiC,react}} = V_p + V_{\text{gr}}\left(1 - \frac{V_m^{\text{SiC}}}{V_m^{\text{gr}}}\right) + V_{\text{pc}}\left(1 - \frac{V_m^{\text{SiC}}}{V_m^{\text{pc}}}\right) \tag{30}$$

With $N_{\text{Si,free}} V_m^{\text{liquid}} = V_{\text{Si,free}}$ we find:

$$\begin{aligned} V_{\text{Si,free}} &= \left(N_X\left(\frac{c_{\text{Si}}}{(1-c_{\text{Si}})} - n\right) - \left(\frac{V_{\text{gr}}}{V_m^{\text{gr}}} + \frac{V_{\text{pc}}}{V_m^{\text{pc}}}\right)\right) V_m^{\text{liquid}} \\ &= \left(\frac{V_{\text{Si}_n X}}{V_m^{\text{Si}_n X}}\left(\frac{(n+1)c_{\text{Si}} - n}{(1-c_{\text{Si}})}\right) - \left(\frac{V_{\text{gr}}}{V_m^{\text{gr}}} + \frac{V_{\text{pc}}}{V_m^{\text{pc}}}\right)\right) V_m^{\text{liquid}} \end{aligned} \tag{31}$$

which allows us to substitute $V_{Si,free}$ in the previous equation. Isolating $V_{\text{Si}_n X}$leads to

$$V_{\text{Si}_n X} = \frac{V_p + V_{\text{gr}}\left(1 - \frac{V_m^{\text{SiC}}}{V_m^{\text{gr}}} + \frac{V_m^{\text{liquid}}}{V_m^{\text{gr}}}\right) + V_{\text{pc}}\left(1 - \frac{V_m^{\text{SiC}}}{V_m^{\text{pc}}} + \frac{V_m^{\text{liquid}}}{V_m^{\text{pc}}}\right)}{\left(1 + \frac{V_m^{\text{liquid}}}{V_m^{\text{Si}_n X}}\left(\frac{(n+1)c_{\text{Si}} - n}{(1-c_{\text{Si}})}\right)\right)} \tag{32}$$

The volume fraction of free silicon becomes then

$$V_{\text{Si,free}} = \left(\frac{V_{\text{Si}_n X}}{V_m^{\text{Si}_n X}}\left(\frac{(n+1)c_{\text{Si}} - n}{(1-c_{\text{Si}})}\right) - \left(\frac{V_{\text{gr}}}{V_m^{\text{gr}}} + \frac{V_{\text{pc}}}{V_m^{\text{pc}}}\right)\right) V_m^{\text{liquid}} \tag{33}$$

For the domain where free carbon is expected, i.e. below the red curve, we proceed analogously. The preform will react with the entering liquid Si-X alloy of with a concentration of c_{Si} in the alloy. The final situation is that all silicon that has entered the preform has either reacted with the carbonaceous phases or is captured in the next stable silicide of the stoichiometry Si_mX.

The final situation will be that the initial volume fraction of the pores, and a fraction of the volume fraction of the carbonaceous phases will be replaced by freshly reacted SiC and Si_mX. Hence,

$$V_p + \Delta V_{\text{gr}} + \Delta V_{\text{pc}} = V_{\text{Si}_m X} + V_{\text{SiC,react}} \tag{34}$$

Similarly to above it can be shown that the fraction, N_{Si}, $\text{SiC}_{\text{react}}$, of silicon atoms being available for reaction with carbonaceous phases is linked to the total number of silicon atoms per volume, N_{Si}, entered by infiltration by

$$N_{\text{Si,SiC react}} = N_{\text{Si}}\left(\frac{(m+1)c_{\text{Si}} - m}{c_{\text{Si}}}\right) \tag{35}$$

Combined with$N_{\text{Si}} = N_{\text{Si,SiC react}} + N_{\text{Si,Si}_m X}$ one finds

$$N_{\text{Si,Si}_m X} = N_{\text{Si,SiC react}} \frac{m(1-c_{\text{Si}})}{(m+1)c_{\text{Si}} - m} \tag{36}$$

The volume fraction of the Si_mX phase can be expressed now as a function of the fraction of silicon atoms having entered the preform by infiltration, and reacted to fresh SiC, $N_{Si,SiC\,react}$, as

$$V_{\text{Si}_m X} = N_{\text{Si,Si}_m X} V_m^{\text{Si}_m X} = N_{\text{Si,SiC react}} \frac{m(1-c_{\text{Si}})}{(m+1)c_{\text{Si}} - m} V_m^{\text{Si}_m X} \tag{37}$$

Similarly, the volume fraction of freshly reacted SiC becomes

$$V_{\text{SiC, react}} = N_{\text{Si,SiC react}} V_m^{\text{SiC}} \tag{38}$$

The fractions the volumes of the carbonaceous phases, ΔV_{gr} and ΔV_{pc} for graphite and pyrolytic carbon, respectively, that react with the silicon are consumed proportional to their atomic concentration in the preform:

$$\Delta V_{\text{gr}} = \frac{V_{\text{gr}}}{\frac{V_{\text{gr}}}{V_m^{\text{gr}}} + \frac{V_{\text{pc}}}{V_m^{\text{pc}}}} N_{\text{Si,SiC react}} \tag{39}$$

and

$$\Delta V_{\text{pc}} = \frac{V_{\text{pc}}}{\frac{V_{\text{gr}}}{V_m^{\text{gr}}} + \frac{V_{\text{pc}}}{V_m^{\text{pc}}}} N_{\text{Si,SiC react}} \tag{40}$$

Expressing all volume fractions, i.e. ΔV_{gr}, ΔV_{pc}, $V_{\text{Si}_m X}$, and $V_{SiC,\,react}$, as a function of $N_{Si,SiC\,react}$ one finds

$$N_{\mathrm{Si,SiC\ react}} = \frac{V_p}{\left(\frac{m(1-c_{\mathrm{Si}})}{(m+1)c_{\mathrm{Si}}-m}V_m^{\mathrm{Si}_m X} + V_m^{\mathrm{SiC}} + \frac{V_{\mathrm{gr}}+V_{\mathrm{pc}}}{\frac{V_{\mathrm{gr}}}{V_m^{\mathrm{gr}}}+\frac{V_{\mathrm{pc}}}{V_m^{\mathrm{pc}}}}\right)} \tag{41}$$

Inserting in the expressions above allows finding the respective volume fractions. We note that for the Si-Zr system, the free silicon volume fraction gets negative when the initial pore volume fraction reaches the blue curve in Fig. 1 from above and so do the volume fractions of the carbonaceous phases if one passes the red line in Fig. 1.

The interest of the calculations presented above is (i) to be able to make a quantitative prediction of what phases and how much of them should be present for a given preform infiltrated with a given alloy when full reaction conversion is reached; and (ii) to assess the observed density after infiltration against a qualified expectation. Both will be used in the chapter on preform infiltration.

4. Modelling pore clogging in a single carbon microchannel

The pore clogging in Si alloy infiltration can be anticipated to happen by two effects. First, by formation of solid SiC in the pore space upon reaction of carbon with liquid silicon, and second, by the precipitation of solid silicides at the infiltration front due to continuous consumption of silicon at the infiltration front by the initial wettable SiC formation and concomitant enrichment of the silicide former. We present here a basic mathematical model to obtain the conditions under which the pore clogging can happen by precipitation of silicides. We make the following simplifying assumptions:

1. The infiltration rate is controlled by the rate of reaction at the triple line and takes a characteristic value for a given temperature.
2. The change in composition of the liquid at the triple line has no influence neither on the growth rate of the SiC layer nor on the triple line velocity (at least as long as the infiltrant is liquid at the triple line).
3. The reaction of some of the silicon in the liquid with the carbon wall does neither lead to changes in the channel geometry nor to reduction of the liquid volume but simply to consumption of Si atoms.
4. The enthalpy of reaction is neglected and the whole process happens at an imposed temperature, T. The increase in local temperature due to heat generated by exothermic reaction between Si and C from the microchannel walls is likely to be very low due to the much faster heat dissipation via carbon walls of microchannel. This however may not be true in bulk preform infiltration scenario.
5. The pore closure due to excessive growth of SiC is not considered here.

The assumptions are valid as long as the channels are relatively wide compared to the thickness of the SiC layer, and if reaction is relatively slow. Also, the propensity of the alloyed transition metals to form silicides is more than that of to form carbides at lower concentrations as seen in our previous study on the wettability of Si-Zr alloy on C and SiC [9]. We use Si-Zr alloy as an example infiltrant but the model is also applicable to other alloying element which can form silicides.

4.1. Development of the model

Consider a rectangular channel of carbon with cross-section we, where w stands for the width and e for the thickness such that $w \gg e$ as shown in Fig. 2. For the purpose of the simplicity, it is assumed that the alloy is already in a liquid state at the time of introduction to the capillary. The microchannel is infiltrated to a length L and the quantity of silicon atoms, n_{Si}, that have been consumed so far by the formation of SiC correspond to a volume of length, λ, taking into account the initial concentration of Si, c_{Si}, and the molar volume. The quantity of zirconium atoms, n_{Zr}, in that same volume are rejected into the liquid behind and diluted in a volume of length, δ, that corresponds to the diffusion length. With the help of the observation from Refs. [10–13], the thickness of the reaction formed SiC layer, $d_{SiC,0}$, can be assumed to evolve according to Eq. (42),

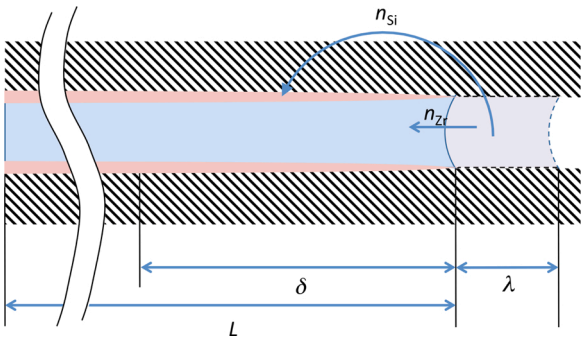

Fig. 2. Schematic of the carbon microchannel with rectangular cross section we filled with the liquid Si-Zr alloy to a length L. The quantity of silicon atoms, n_{Si}, that have been consumed so far by the formation of SiC corresponds to a volume of length, λ, taking into account the initial concentration of Si, c_{Si}, and the molar volume. The quantity of zirconium atoms, n_{Zr}, in that same volume are rejected into the liquid behind and diluted in a volume of length, δ, that corresponds to the diffusion length.

$$d_{\mathrm{SiC}} = d_{\mathrm{SiC},0} exp\left[\frac{-Q_{\mathrm{SiC}}}{\mathrm{RT}}\right] t^{\frac{1}{n}} \tag{42}$$

with $d_{SiC,0}$ the prefactor, Q_{SiC} the activation energy of the SiC growth, t is the time since the beginning of the growth, and R and T are the gas constant and the temperature, respectively. For the derivation, we keep n as a parameter since there are in the literature various descriptors for the growth kinetics of the SiC layer, with n sometimes equal to 2 and sometimes equal to 4. We further assume, as stated in the simplifying assumptions, that the velocity of ingress, v, is a fixed value for a given temperature, and can be expressed as a function of temperature as

$$v = v_{\mathrm{tr}} = v_0 exp\left[\frac{-Q_{\mathrm{triple}}}{\mathrm{RT}}\right] \tag{43}$$

with v_0 the prefactor and Q_{triple} the activation energy of the triple line reaction, while R and T are as usual the gas constant and the temperature, respectively. The diffusion length, δ, is given as a function of the time, t, and the diffusion coefficient, $D_{Si/Zr}$ as

$$\delta = \sqrt{D_{\mathrm{Si/Zr}} t} \tag{44}$$

The diffusion coefficient can again be written as a function of temperature, T, in terms of a prefactor $D_{Si/Zr,0}$ and an activation energy, Q_{diff}, as

$$D_{\mathrm{Si/Zr}} = D_{\frac{\mathrm{Si}}{\mathrm{Zr},0}} exp\left[\frac{-Q_{\mathrm{diff}}}{\mathrm{RT}}\right] \tag{45}$$

The quantity of silicon atoms, that has been consumed when the triple line arrives at a position L in the channel is given by

$$n_{\mathrm{Si}}^{\mathrm{SiC}} = \frac{2(e+w)\mathrm{Ld}_{\mathrm{SiC},0} exp\left[\frac{-Q_{\mathrm{SiC}}}{\mathrm{RT}}\right] t^{\frac{1}{n}}}{V_m^{\mathrm{SiC}}} \tag{46}$$

From this we can deduce the equivalent length, λ, of alloy that is consumed in the formation of SiC as

$$\lambda = \frac{2(e+w)\mathrm{Ld}_{\mathrm{SiC},0} exp\left[\frac{-Q_{\mathrm{SiC}}}{\mathrm{RT}}\right] t^{\frac{1}{n}}}{\mathrm{ew}} \frac{V_m^{\mathrm{liquid}}}{V_m^{\mathrm{SiC}}} \frac{1}{c_{\mathrm{Si},0}} \tag{47}$$

and the reduced length, λ_{Zr}, that corresponds to the length filled by all the zirconium atoms left behind becomes:

$$\lambda_{Zr} = \frac{2(e+w)\mathrm{Ld}_{\mathrm{SiC},0} exp\left[\frac{-Q_{\mathrm{SiC}}}{\mathrm{RT}}\right] t^{\frac{1}{n}}}{\mathrm{ew}} \frac{V_m^{\mathrm{liquid}}}{V_m^{\mathrm{SiC}}} \frac{\left(1-c_{\mathrm{Si},0}\right)}{c_{\mathrm{Si},0}} \tag{48}$$

under the assumption that the partial molar volumes of silicon and zirconium atoms are identical. The zirconium atoms contained in that volume are then mixed with the atoms contained in a volume given by $ew(\delta - \lambda_{Zr})$ with initial composition $c_{Si,0}$. The total volume of these two volumes is then again $ew\delta$. The silicon concentration in that volume, c_{Si}, can be calculated as

$$c_{\mathrm{Si}} = \frac{\delta - \lambda_{\mathrm{Zr}}}{\delta} c_{\mathrm{Si},0} \tag{49}$$

There is a critical value of zirconium enrichment and, hence, silicon concentration, $c_{\mathrm{Si}}^{\mathrm{crit}}$, at which the formation of zirconium silicide will block the flow of liquid and stop the infiltration. The accumulated virtual pure zirconium length, λ_{Zr}, takes the value

$$\lambda_{\mathrm{Zr}} = \frac{\delta\left(c_{\mathrm{Si},0} - c_{\mathrm{Si}}^{\mathrm{crit}}\right)}{c_{\mathrm{Si},0}} \tag{50}$$

whence

$$\frac{\delta\left(c_{\mathrm{Si},0} - c_{\mathrm{Si}}^{\mathrm{crit}}\right)}{\left(1-c_{\mathrm{Si},0}\right)} = \frac{2(e+w)\mathrm{Ld}_{\mathrm{SiC},0} exp\left[\frac{-Q_{\mathrm{SiC}}}{\mathrm{RT}}\right] t^{\frac{1}{n}}}{\mathrm{ew}} \frac{V_m^{\mathrm{liquid}}}{V_m^{\mathrm{SiC}}} \tag{51}$$

With $e \ll w$ we can write

$$\frac{\left(c_{\mathrm{Si},0} - c_{\mathrm{Si}}^{\mathrm{crit}}\right)}{\left(1-c_{\mathrm{Si},0}\right)} \frac{V_m^{\mathrm{SiC}}}{V_m^{\mathrm{liquid}}} = \frac{2\mathrm{Ld}_{\mathrm{SiC},0} exp\left[\frac{-Q_{\mathrm{SiC}}}{\mathrm{RT}}\right] t^{\frac{1}{n}}}{e\delta} \tag{52}$$

The time over which the growth of the SiC layer affects the Si concentration of the volume under consideration of length, δ, from the infiltration front is $t = \frac{\delta}{v}$. Inserting this in the equation above we find:

$$\frac{\left(c_{\mathrm{Si},0} - c_{\mathrm{Si}}^{\mathrm{crit}}\right)}{\left(1-c_{\mathrm{Si},0}\right)} \frac{V_m^{\mathrm{SiC}}}{V_m^{\mathrm{liquid}}} = \frac{2\mathrm{Ld}_{\mathrm{SiC},0} exp\left[\frac{-Q_{\mathrm{SiC}}}{\mathrm{RT}}\right] \left(\frac{\delta}{v}\right)^{\frac{1}{n}}}{e\delta} = \frac{2\mathrm{Ld}_{\mathrm{SiC},0} exp\left[\frac{-Q_{\mathrm{SiC}}}{\mathrm{RT}}\right]}{e\delta^{\frac{n-1}{n}} v^{\frac{1}{n}}} \tag{53}$$

The diffusion length, δ, itself is linked to the total time the infiltration has taken place, the latter being given by $\frac{L}{v}$, by:

$$\delta = \sqrt{D_{\mathrm{diff}} \frac{L}{v}} \tag{54}$$

Inserting this value of δ in the above equation, we find:

$$\begin{aligned}
\frac{\left(c_{\mathrm{Si},0} - c_{\mathrm{Si}}^{\mathrm{crit}}\right)}{\left(1-c_{\mathrm{Si},0}\right)} \frac{V_m^{\mathrm{SiC}}}{V_m^{\mathrm{liquid}}} &= \frac{2\mathrm{Ld}_{\mathrm{SiC},0} exp\left[\frac{-Q_{\mathrm{SiC}}}{\mathrm{RT}}\right]}{e\left(D_{\mathrm{diff}} L\right)^{\frac{n-1}{2n}} v^{\frac{1}{n}-\frac{n-1}{2n}}} \\
&= \frac{2\mathrm{Ld}_{\mathrm{SiC},0} exp\left[\frac{-Q_{\mathrm{SiC}}}{\mathrm{RT}}\right]}{e\left(D_{\mathrm{diff}} L\right)^{\frac{n-1}{2n}} v^{\frac{3-n}{2n}}} \\
&= \frac{2L^{\frac{n+1}{2n}} d_{\mathrm{SiC},0} exp\left[\frac{-Q_{\mathrm{SiC}}}{\mathrm{RT}}\right]}{eD_{\mathrm{diff}}{}^{\frac{n-1}{2n}} v^{\frac{3-n}{2n}}} \\
&= \frac{2L^{\frac{n+1}{2n}} d_{\mathrm{SiC},0} exp\left[\frac{-Q_{\mathrm{SiC}}}{\mathrm{RT}}\right]}{eD_{\mathrm{diff},0}{}^{\frac{n-1}{2n}} exp\left[\frac{-(n-1)Q_{\mathrm{diff}}}{2\mathrm{nRT}}\right] v_0{}^{\frac{3-n}{2n}} exp\left[\frac{-(3-n)Q_{\mathrm{triple}}}{2\mathrm{nRT}}\right]}
\end{aligned} \tag{55}$$

Isolating the length of infiltration, L, at which the critical concentration is obtained at the infiltration front leads to

$$L = \left[\frac{\left(c_{\mathrm{Si},0} - c_{\mathrm{Si}}^{\mathrm{crit}}\right)}{\left(1-c_{\mathrm{Si},0}\right)} \frac{V_m^{\mathrm{SiC}}}{V_m^{\mathrm{liquid}}} \frac{e\ D_{\mathrm{diff},0}{}^{\frac{n-1}{2n}}}{2 v_0{}^{\frac{n-3}{2n}} d_{\mathrm{SiC},0}} exp\left[\frac{2\mathrm{nQ_{SiC}} - (n-1)Q_{\mathrm{diff}} - (3-n)Q_{\mathrm{triple}}}{2\mathrm{nRT}}\right]\right]^{\frac{2n}{n+1}} \tag{56}$$

This is a closed expression (Eq. (56)) for the length, L, over which the infiltration should be able to take place before blocking by the formation of silicide is observed. All important system parameters, i.e. channel dimension, growth and diffusion kinetics and infiltration rate enter into the equation, as well as the initial concentration of the alloy.

4.2. Implications of the model

In Fig. 3(a), an example of the effect of temperature on infiltration length of a carbon microchannel with a rectangular cross section and of thickness of 10 μm, infiltrated by Si-8 at.% Zr alloy, is plotted using Eq. (56). The values for the parameters used in the model are taken from Refs. [14–17]. The value $d_{SiC,0}$ was calculated from the experimental observations of Voytovych et al. [13]. The value of $c_{\mathrm{Si}}^{\mathrm{crit}}$ was taken as per the Si-Zr phase diagram considering the concentration of Zr is such that 80% of the phase fraction at given temperature is solid using lever rule, which corresponds to approximately 27.8 at.% Zr below peritectic temperature of 1620 °C, and increases to 43.6 at.% Zr above 1620 °C. The calculation used a value of $n = 2$:

$$\begin{aligned}
V_m^{\mathrm{SiC}} &= 1.25 \times 10^{-5}\ \mathrm{m^3/mol} \\
V_m^{\mathrm{liquid}} &= 1.31 \times 10^{5}\ \mathrm{m^3/mol} \\
D_{\mathrm{diff},0} &= 15 \times 10^{-9}\ \mathrm{m^2/s} \\
v_0 &= 2 \times 10^{-4}\ m/s \ \text{ at } \ 1500\,^{\circ}\mathrm{C} \\
d_{\mathrm{SiC},0} &= 9 \times 10^{-6}\ \mathrm{m} \\
Q_{\mathrm{SiC}} &= 200 \times 10^{3}\ \mathrm{J/mol} \\
Q_{\mathrm{diff}} &= 28 \times 10^{3}\ \mathrm{J/mol} \\
Q_{\mathrm{triple}} &= 185 \times 10^{3}\ \mathrm{J/mol}
\end{aligned}$$

The triple line velocity indicated here is significantly larger, by a factor of 5, roughly, than the observed triple line velocities in sessile drop spreading experiments. While the latter could be considered as a good approximative indicator for the spreading rate on inner surfaces of preforms or microchannel experiments, the observed infiltration distances in pure Si experiments set a lower limit to triple line velocity. It is roughly that lower limit that has been chosen here. On the other hand, the thermal activation energy of the triple line velocity, Q_{triple}, has been derived from observed spreading rates in sessile drop experiments at different temperatures [16]. From Fig. 3(a), one could conclude that the infiltration length decreases with increase in process temperature for a near eutectic concentration of alloy. The sudden change in infiltration length for the process temperature above the peritectic temperature is due to the fact that the solid fraction is much lower above the peritectic temperature for a given composition.

Fig. 3(b) shows the infiltration length as a function of initial Zr concentration for a 10 μm carbon microchannel at 1500 °C. One can clearly see that with increasing Zr concentration the infiltration length reduces and for a certain threshold value (~33 at.% Zr in this case) where the alloy itself is solid at the infiltration temperature resulting in no infiltration. Another important thing to notice is the very high infiltration length as the Zr concentration closes to zero. This is due to the fact that in developing the leading equation reflected in the graph we did only consider the clogging by silicide formation at the infiltration front and not clogging at the rear of the infiltration by reaction formed SiC.

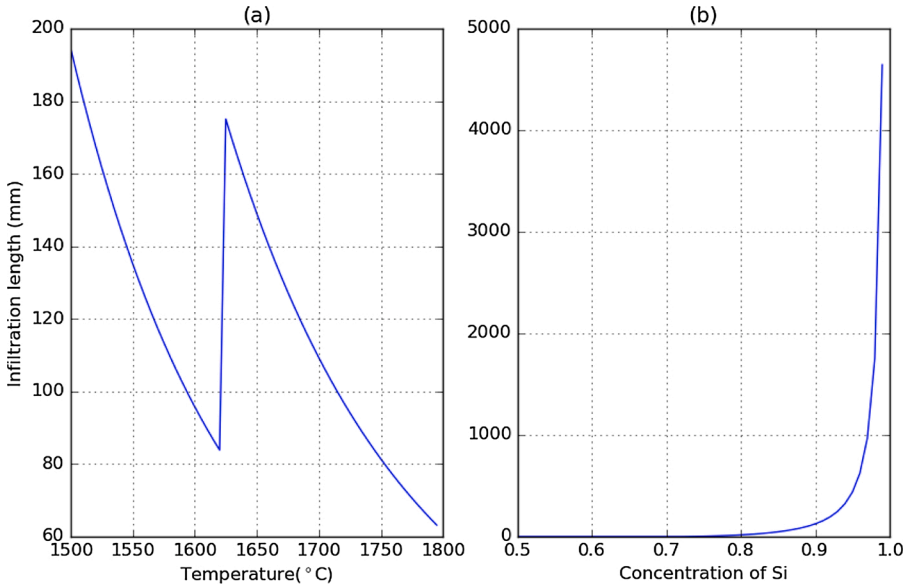

Fig. 3. Infiltration length calculated using Eq. (56) for a carbon microchannel with a rectangular cross section and of thickness of 10 μm (a) with increasing temperature, infiltrated by Si-8 at.% Zr alloy (b) infiltration length as function of initial Si fraction at 1500 °C.

5. Extension of the model to preform infiltration

The simple straight rectangular capillary is a good descriptor of the single microchannel experiments but not for a preform as used in typical infiltration experiments. Those preforms deviate in two points from the simple microchannel: (i) the geometry is no longer a straight infiltration capillary of fixed cross-section, and (ii) parts of the surface of the channels are provided by existing SiC in the preform. To account for these features we have to adapt the model. This is outlined in the following.

5.1. Accounting for arbitrary capillary shape

$$v_{inf} = v_{tr}\left\langle cos\alpha \right\rangle = \xi v_{tr} = \xi v_0 exp\frac{-Q_{triple}}{RT} \tag{57}$$

An arbitrary pore channel cross section leads to two changes in the equations developed above: (i) the surface-to-volume ratio changes, which has an effect on the amount of Si consumed and hence the concentration of the alloying element close to the infiltration front, and (ii) the velocity of the triple line is now no longer only parallel to the infiltration direction that is on first order perpendicular to the outer surface but locally meanders around that infiltration direction vector. The situation is schematically depicted in Fig. 4. The changing of the surface-to-volume ratio from bottle-necks to larger spaces can be accounted for by a characteristic capillary radius, R^*, that is chosen such that its specific surface is equal to that of a preform under consideration. The deviation of the triple line velocity vector, v_{tr}, with regard to the infiltration direction is taken care of by the vector average of the triple line velocity vector, $v_{inf} = v_{tr} = v_{tr}cos\alpha$, where α is the angle between the local triple line velocity and the macroscopic infiltration direction. We hence write:

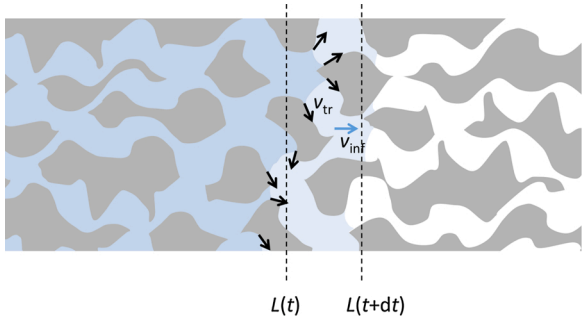

Fig. 4. Schematic representation of the infiltration in a real preform. The infiltration velocity, v_{inf}, is no longer equal to the triple line velocity as in the microchannel model.

Note that the factor ξ accounts for the local surface inclination coming from both, the local change in channel cross-section and the tortuosity of the infiltration path.

5.2. Accounting for the presence of SiC particles

The SiC particles present in the preform will change the surface available for reaction. The fraction of the preform surface that has to react in order to allow advancing of the infiltration front is given by a factor, ϕ. In first approximation, one could assume that ϕ is equal to one minus the volume fraction of SiC, $V_{p,SiC}$, in the solid of the preform. It is, however, expected that this is a lower limit given the fact that the graphite and SiC particles are mixed with the phenolic resin and hence both the SiC particles and the graphite particles are at least in part covered with a thin film of pyrolytic carbon. Therefore, the factor ϕ is most likely contained by $1 - V_{p,SiC} \leq \phi \leq 1$. The rate of infiltration is not expected to change since the parts of the surface composed of carbonaceous material will only allow the advancing of the infiltration front at the rate that the interface between liquid and preform is converted into wetted SiC. We consider here that $\langle cos\alpha \rangle$ is the same for the surfaces formed by SiC as for those formed by carbonaceous material.

5.3. Changes to the guiding equations

The changes to the guiding equations of the infiltration model of the microchannel are outlined in the following. The infiltration velocity, $v_{inf} = \frac{dL}{dt}$, becomes now a fraction of the triple line velocity, v_{tr}, but remains proportional to it, as outlined above. The quantity of silicon atoms, that has been consumed when the triple line arrives at a position L in the preform is now given by

$$n_{Si}^{SiC} = \frac{2\pi R^* \phi L d_{SiC,0} exp\left[\frac{-Q_{SiC}}{RT}\right] t^{\frac{1}{n}}}{V_m^{SiC}} \tag{58}$$

where the factor, ϕ, accounts for the reduced consumption of Si due to the presence of SiC particles and persists in the development as presented for the microchannel. The geometrical change from $2(e+w)$ for the surface and ew for the cross section (both for a unity of length) to the corresponding values of $2\pi R^*$ and πR^{*2}, respectively, of the equivalent capillary as defined above, leads to a replacement of the term $2/e$ by $2/R^*$. If all these changes are introduced, the guiding equation determining the infiltration length becomes:

$$L = \left[\frac{(c_{Si,0} - c_{Si}^{crit})}{(1 - c_{Si,0})} \frac{V_m^{SiC}}{V_m^{liquid}} \frac{R^*}{2\phi} \frac{D_{diff,0}^{\frac{n-1}{2n}}}{\xi^{\frac{n-3}{2n}} v_0^{\frac{n-3}{2n}} d_{SiC,0}} exp\left[\frac{2nQ_{SiC} - (n-1)Q_{diff} - (3-n)Q_{triple}}{2nRT}\right]\right]^{\frac{2n}{n+1}} \tag{59}$$

5.4. The equivalent pore radius of the preform

The equivalent radius for the porous preform can be determined as follows: Be a_i the specific surface area per weight in $m^2\,g^{-1}$ of the particle type i. The specific surface area per volume, α_i, is then:

$$\alpha_i = a_i \rho_i \tag{60}$$

with ρ_i the density of particle type i in $g\,m^{-3}$ The inner surface per volume of the preform is the sum of the products of volume fraction of the particles of type i times their specific surface area per volume, and it must be equal to the volume fraction of equivalent cylindrical channels with radius R^* times their specific surface area. For the latter we find:

$$\alpha_{eq.\,cyl.} = \frac{2\pi R^*}{\pi R^{*2}} = \frac{2}{R^*} \tag{61}$$

As said before, that must be equal to the specific surface area of the particles:

$$V_p \alpha_{eq.\,cyl.} = \frac{2V_p}{R^*} = V_{gr}\alpha_{gr} + V_{SiC}\alpha_{SiC} \tag{62}$$

whence

$$R^* = \frac{2V_p}{V_{gr}\alpha_{gr} + V_{SiC}\alpha_{SiC}} \tag{63}$$

Hence, for every preform, R^* can be calculated based on the particles that are included in the preform. For simplicity's sake we neglect the pyrolysed carbon from the phenolic resin.

5.5. Implication of the model to preform infiltration

In Fig. 5(a), the infiltration length is plotted with increasing infiltration temperature for a SiC-C preform with $R^* = 0.5\,\mu m$, infiltrated by Si-8 at.% Zr alloy, using Eq. (59). The value of $\phi = 0.5$ and $\xi = 1/3$ were used for the calculations. The rest of the parameters are same as mentioned before in the infiltration length calculation for microchannel. As expected this also shows the similar trend of decreasing infiltration depth with increasing temperature and sudden increase in the infiltration depth at peritectic temperature. In Fig. 5(b),the infiltration length for a SiC-C preform with $R^* = 0.5\,\mu m$ as a function of initial Zr

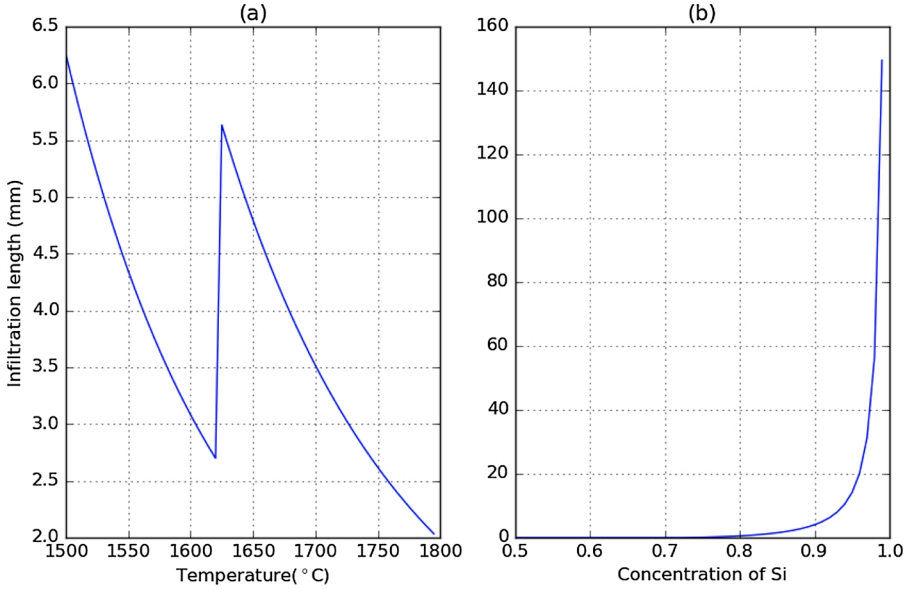

Fig. 5. Infiltration length calculated using Eq. (59) for a SiC-C preform having $R^* = 0.5\,\mu m$ (a) with increasing temperature, infiltrated by Si-8 at.% Zr alloy (b) with increasing Si fraction infiltrated at 1500 °C.

concentration in the alloy is also plotted using Eq. (59) for a processing temperature of 1500 °C. Also, a similar trend can be observed where the infiltration depth is decreasing with increasing initial Zr concentration in the alloy. The values of the infiltration length where initial Zr concentration is very low have to be taken with a grain of salt: it could very well be that the infiltration is stopped earlier by the clogging of the entrance channels due to the formation of SiC, which was however not considered here. Overall, the model for adequate pore fraction combined with the model for pore clogging in preforms by silicide formation at the infiltration front highlights the concurring interest in the choice of the right alloy composition: on the one hand, larger silicide former contents in the alloy increase the latitude in adequate porosity levels in the preform, as illustrated in Fig. 1 by the increasing distance between the red and the blue line as the concentration of the silicide forming alloying element increases. On the other hand, increasing the concentration of the silicide forming element in the infiltrating alloy reduces the expected infiltration length due to solid silicide precipitation at the infiltration front, as shown in Fig. 5.

The parameters to play with are then the particle size of the constituents of the preform and the volume fraction of carbonaceous material in the preform. Both are likely to affect the equivalent radius R^* and the coverage parameter ϕ. Combinations with large particles and low carbonaceous phase content (and concomitantly, low pore volume fraction in the preform) seem the most promising that could also accommodate larger silicide former concentrations in the infiltrant. At the same time, such a parameter set would also reduce the risk of clogging due to reactive SiC formation. The limit in this direction is set by the length scale over which reaction conversion can be obtained.

6. Differential model for non-isothermal infiltration experiments

In our experimental study [5,6] and in many practical infiltration settings the infiltration is not isothermal but starts as soon as the liquid silicon or silicon alloy is in contact with the preform. Many of the intervening quantities in the isothermal model are however temperature dependent and will change with the changes in temperature during infiltration. In all generality, closed form expression for the infiltration will no longer be available. We develop for the non-isothermal case hence a differential scheme that can be numerically integrated.

6.1. Formulation of the model

We start with the number of Si atoms, $n_{\mathrm{Si}}^{\mathrm{SiC}}$, that have been consumed for the formation of wettable SiC from the volume element extending by the diffusion length, δ, from the infiltration front back into the liquid at time t. Similarly, to Eq. (46), we find:

$$n_{\mathrm{Si}}^{\mathrm{SiC}}(t) = \frac{2(e+w)L(t)\theta_{\mathrm{SiC},0} exp\left[\frac{-Q_{\mathrm{SiC}}}{\mathrm{RT}(t)}\right]\left(\frac{\delta(t)}{v(t)}\right)^{\frac{1}{n}}}{V_m^{\mathrm{SiC}}} \tag{64}$$

The same quantity a moment dt later, $n_{\mathrm{Si}}^{\mathrm{SiC}}(t+\mathrm{d}t)$, is

$$n_{\mathrm{Si}}^{\mathrm{SiC}}(t+\mathrm{d}t) = \frac{2(e+w)L(t+\mathrm{d}t)\theta_{\mathrm{SiC},0} exp\left[\frac{-Q_{\mathrm{SiC}}}{\mathrm{RT}(t+\mathrm{d}t)}\right]\left(\frac{\delta(t+\mathrm{d}t)}{v(t+\mathrm{d}t)}\right)^{\frac{1}{n}}}{V_m^{\mathrm{SiC}}} \tag{65}$$

We assume that the only rapidly changing entity is the infiltration length, L, and hence write

$$n_{\mathrm{Si}}^{\mathrm{SiC}}(t+\mathrm{d}t) - n_{\mathrm{Si}}^{\mathrm{SiC}}(t) = \frac{2(e+w)(L(t+\mathrm{d}t)-L(t))d_{\mathrm{SiC},0} exp\left[\frac{-Q_{\mathrm{SiC}}}{\mathrm{RT}(t)}\right]\left(\frac{\delta(t)}{v(t)}\right)^{\frac{1}{n}}}{V_m^{\mathrm{SiC}}} \tag{66}$$

and with $L(t+\mathrm{d}t) - L(t) = v(t)\mathrm{d}t$

$$\frac{\mathrm{d}n_{\mathrm{Si}}^{\mathrm{SiC}}(t)}{\mathrm{d}t} = \frac{2(e+w)v(t)d_{\mathrm{SiC},0} exp\left[\frac{-Q_{\mathrm{SiC}}}{\mathrm{RT}(t)}\right]\left(\frac{\delta(t)}{v(t)}\right)^{\frac{1}{n}}}{V_m^{\mathrm{SiC}}} \tag{67}$$

The equivalent channel length of liquid, λ, as used previously, becomes:

$$\lambda(t) = \int_0^t \frac{\mathrm{d}n_{\mathrm{Si}}^{\mathrm{SiC}}(t)}{\mathrm{d}t}\mathrm{d}t\ \frac{V_m^{\mathrm{liquid}}}{\mathrm{ew}}\ \frac{1}{c_{\mathrm{Si},0}} \tag{68}$$

and for λ_{Zr} as well as the silicon concentration in the volume element within δ of the infiltration front we find analogously to above

$$\lambda_{\mathrm{Zr}}(t) = \int_0^t \frac{\mathrm{d}n_{\mathrm{Si}}^{\mathrm{SiC}}(t)}{\mathrm{d}t}\mathrm{d}t\ \frac{V_m^{\mathrm{liquid}}}{\mathrm{ew}}\ \frac{(1-c_{\mathrm{Si},0})}{c_{\mathrm{Si},0}} \tag{69}$$

and

$$c_{\mathrm{Si}}(t) = \frac{\delta(t)-\lambda_{\mathrm{Zr}}(t)}{\delta(t)}c_{\mathrm{Si},0} \tag{70}$$

The diffusion length, δ, is simply related to the time, t, since the infiltration started

$$\delta(t) \approx \sqrt{D_{\frac{\mathrm{Si}}{\mathrm{Zr},0}} exp\left[\frac{-Q_{\mathrm{diff}}}{\mathrm{RT}(t)}\right]t} \tag{71}$$

accepting some approximation, given that the temperature itself is also a function of time. The triple line velocity, $v(t)$, will also vary due to the variation of temperature with time:

$$v(t) = v_0 exp\left[\frac{-Q_{\mathrm{triple}}}{\mathrm{RT}(t)}\right] \tag{72}$$

Lastly, the actual position of the triple line, $L(t)$, can be found by integration of the triple line velocity:

$$L(t) = \int_0^t v(t)\mathrm{d}t \tag{73}$$

The time temperature history, $T(t)$, can be arbitrarily set. Typically, the infiltration will start when T reaches the melting temperature of the alloy. At that point, $t = 0$. Once the silicon concentration reaches its critical value, where silicide formation will stop the further advancing of the triple line, the triple line velocity will go to zero. That is, however, not necessarily the end of the infiltration process: as time goes on, the diffusion length will increase. Since at the same time the value of λ_{Zr} stagnates according to Eq. (69), diffusion will eventually increase the Si concentration at the infiltration front again and allow further ingress, but at a slower rate. The condition for the triple line velocity becomes then

$$v(t) = \begin{cases} v_0 exp\left[\frac{-Q_{\mathrm{triple}}}{\mathrm{RT}(t)}\right] & \text{for } c_{\mathrm{Si}} < c_{\mathrm{Si}}^{\mathrm{crit}} \\ 0 & \text{else} \end{cases} \tag{74}$$

The result of the numerical integration of such a non-isothermal infiltration is shown in Fig. 6, for an infiltration run with a continuous heating ramp of 1500 °C/h up to 1500 °C, 1 min hold and natural cool down after the furnace had been switched off. Several domains can be recognised in the modelled curve: in the blue region in Fig. 6, the infiltrated length increases more than proportionally with time due to the fact that the infiltration velocity is increasing with temperature. At the transition between the blue and the green domain, the clogging condition $c_{Si} < c_{Si,crit}$ is reached and the triple line advances only because the diffusion brings constantly silicon to the triple line (or in other words Zr is transported away from the triple line). There is a dynamic equilibrium between enrichment in Zr due to advancing of the triple line and reduction of Zr due to diffusion. Once the maximum temperature is

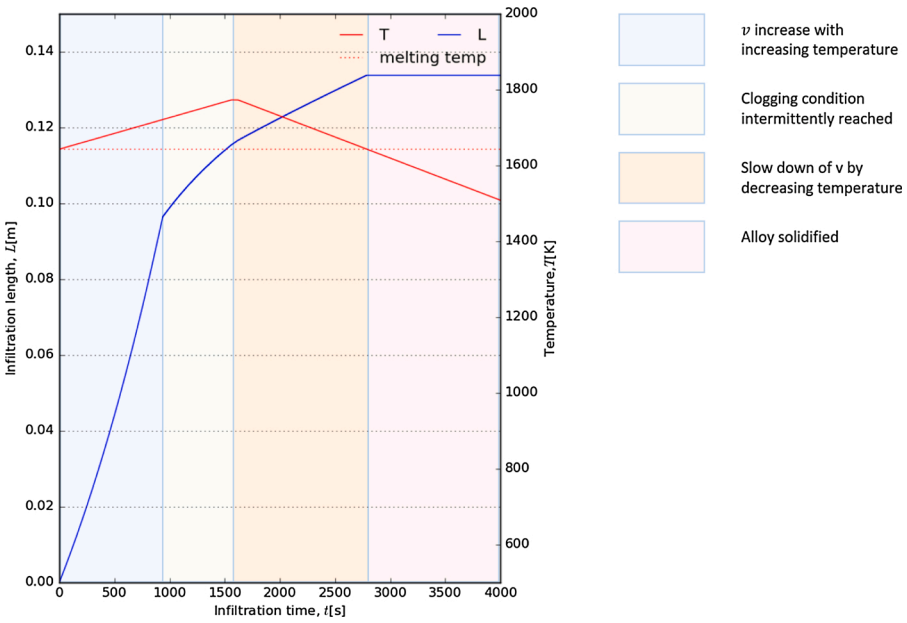

Fig. 6. Evolution of infiltration length, L, and temperature in a non-isothermal infiltration experiment of a Si-8 at.% Zr alloy into a microchannel of 10 μm thickness. At the beginning the infiltration accelerates since the reaction at the triple line is thermally activated. The change in slope in the green region comes by since the clogging condition $c_{Si} < c_{Si,crit}$ is reached but continuously alleviated by the diffusion of Si to the triple line. After having reached the maximum temperature, the triple line velocity stagnates, yet remains controlled by the Si diffusion regime. In the red domain the triple line is stalled due to solidification of the alloy. (For interpretation of the references to colour in this figure legend, the reader is referred to the web version of this article.)

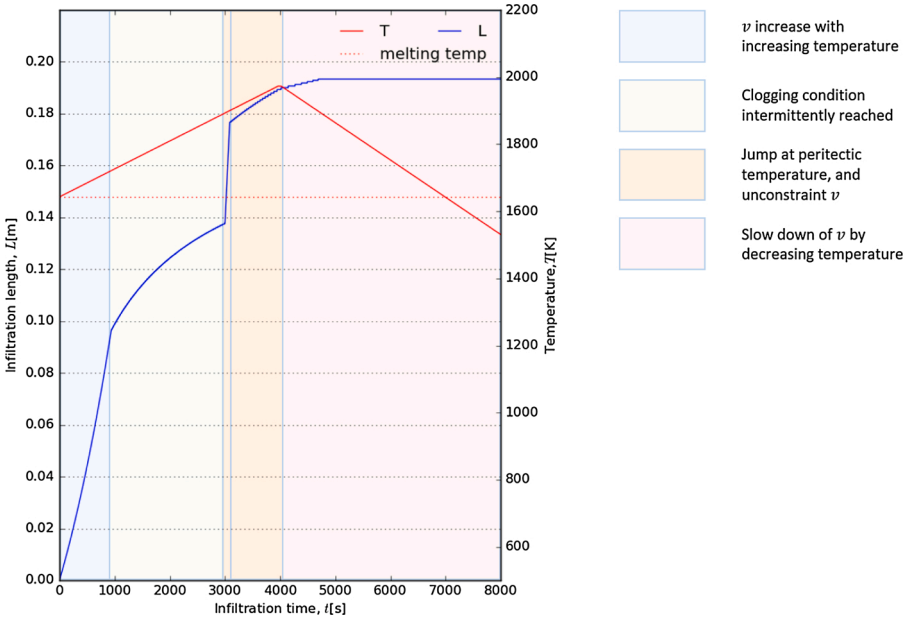

Fig. 7. Evolution of infiltration length, L, and temperature in a non-isothermal infiltration experiment of a Si-8 at.% Zr alloy into a microchannel of 10 μm thickness. As in the example at 1500 °C the infiltration accelerates in the beginning due to thermal activation. The change in slope in the green region comes by since the clogging condition $c_{Si} < c_{Si,crit}$ is reached but continuously alleviated by the diffusion of Si to the triple line. At the peritectic temperature, the critical silicon concentration takes a jump and the triple line is again at its unconstrained speed. After having reached the maximum temperature, the triple line velocity stagnates, yet remains controlled by the Si diffusion regime.

reached, the furnace is shut off, the dynamic equilibrium persists until the solidification temperature is reached where all infiltration comes to a halt.

It is instructive to model the same process for the case that the temperature is raised to 1700 °C as shown in Fig. 7. There are similar domains observed as at 1500 °C. The notable difference comes when the temperature reaches 1893 K (1620 °C), the peritectic temperature of formation of $ZrSi_2$. At that temperature, the critical silicon concentration takes a jump. In the present modelling the critical Si concentration has been 0.73 for temperatures below 1893 K and 0.57 for temperatures above. Compared to the infiltration with maximum temperature 1500 °C, the infiltration length reaches higher values due to the combination of the longer time at high temperature, which increases the diffusion length, and the lower critical silicon concentration at the maximum temperature of the process. The chosen critical composition in the present case corresponds to 80% of solid phase at the eutectic temperature and the peritectic temperature, respectively for temperatures below and above the peritectic temperature. Alternatively, the critical composition could be chosen as that corresponding to an arbitrary fraction of solid at each temperature. The critical silicon concentration in the liquid would also then take a jump at the peritectic temperature except for the case when the solid fraction is chosen as very close to 0. It is instructive to compare the non-isothermal model to the isothermal model with the explicit expression of L as a function of the processing parameters. It turns out that the isothermal model predicts only the infiltration length achieved in the blue regime, i.e. the one until

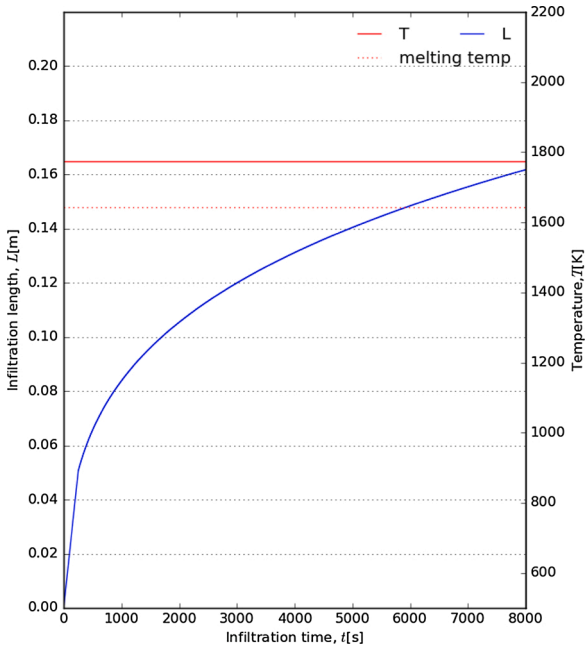

Fig. 8. Evolution of infiltration length, L, with the differential scheme developed for the non-isothermal case applied to the isothermal case by setting the heating rate to 0 and the starting temperature to the isothermal temperature.

the critical composition is reached for the first time. The closed form, and the lack of consideration that the flow condition recovers thanks to diffusion once the triple line has come to a halt, are the main cause for this.

We can of course model the isothermal case by the differential approach of the non-isothermal model by taking a starting temperature identical to the isothermal temperature and choosing a heating ramp of 0 K/h. The results of this are shown in Fig. 8. It can be seen that the infiltration length goes, under the influence of diffusion, way above the value evaluated with the explicit scheme.

The non-isothermal model developed for the single microchannel infiltration can naturally also be extended to be used for the preform infiltration experiments along the lines outlined above for the isothermal case.

6.2. Limits of the differential model

The diffusion mediated ingress appearing in the differential model has to be taken with a grain of salt: In the formulation of the model, it has been assumed that silicon is only consumed while the triple line is advancing, leading us to the statement that λ_{Zr} stagnates when the triple line is at rest. When the triple line comes to a halt, however, there is still some silicon consumed by the continuing of the reaction to SiC, albeit at a (rapidly) decreasing rate as the arrest time increases. This will lead to a slower advancing rate in the diffusion controlled regime than obtained by the current formulation and most likely results in a terminal arrest of the infiltration front and not to a "creeping" advancement of the infiltration front above all limits for long enough times. Including this in the numerical scheme would, however, require a complicated case distinction of silicon consumption between the situation where the triple line moves or is at rest and also a change in formulation at restart of the movement of the triple line. We limit ourselves here to state that the infiltration length shown in Fig. 6 obtained by diffusion mediated ingress is an overestimation and that the real infiltration length expected is somewhere in between the length achieved when the triple line comes first to a halt and the diffusion mediated infiltration length calculated for a given processing time at high temperatures.

A second limitation is that the diffusion length is constantly updated to the new temperature in the non-isothermal model. Upon increasing the temperature this will always lead to an overestimation of the actual diffusion length because diffusion did not operate all along at the (high) current temperature but evolved somewhat more slowly, which made us call Eq. (71) an approximation. The second effect of this updated diffusion length is that as temperature decreases in the non-isothermal model, the diffusion length calculation is subjected to a competition between increase in time (leading to a longer diffusion length) and reduction in diffusion coefficient by reduced thermal activation (leading to a shorter diffusion length). If the net outcome of this competition is a shortening of the diffusion length, this will decrease artificially the concentration of silicon at the infiltration front by virtue of Eq. (70). This leads to the situation that the silicon concentration is increasingly above the critical concentration and continues to increase as temperature decreases. This is the reason why the infiltration length comes to a halt in the modelling shown in 7 albeit the solidification temperature is not yet reached.

7. Conclusion

Analytical models describing infiltration kinetics, porous preform requirements, alloy composition, processing temperature and resulting phases in the reactive infiltration of porous carbonaceous preforms by Si alloys were developed.

- An analytical model for correctly evaluating the adequate pore volume fraction by taking into account the presence of silicide formers, as well as a model to predict theoretical density and phases present after infiltration based on preform composition and preform porosity, was devised. The analytical model's treatment is valid for an extensive range of silicide formers.
- The model showed that an increase in graphite mass fraction in the SiC-C preforms shifted the range of preform porosity leading to composites formed by SiC and silicides to higher values. A porosity above this range results in residual Si, and a porosity below this range results in unreacted graphite.
- For the first time, an analytical model was developed for pore channel closure due to alloying element enrichment at the infiltration front, both for individual straight channels and tortuous porosity under isothermal and non-isothermal processing conditions.
- For the SiC/C preforms, an effective pore radius was calculated in terms of the SiC and graphite powder's specific surface area.
- In isothermal conditions, the infiltration length decreases with increasing temperature, while in the non-isothermal condition, in a particular scenario, higher infiltration lengths can be reached.

Declaration of Competing Interest

The authors report no declarations of interest.

Acknowledgment

The financial support for this research by the Swiss National Science Foundation, SNSF, in the framework of the SIMEA project No. 200021_163017 is gratefully acknowledged.

References

[1] W. Krenkel, Cost effective processing of CMC composites by melt infiltration (LSI-process), Ceramic Engineering and Science Proceedings (2001) 443–454, https://doi.org/10.1002/9780470294680.ch52, book section 52.
[2] P. Sangsuwan, J.A. Orejas, J.E. Gatica, S.N. Tewari, M. Singh, Reaction-bonded silicon carbide by reactive infiltration, Ind. Eng. Chem. Res. 40 (23) (2001) 5191–5198, https://doi.org/10.1021/ie001029e.
[3] W.B. Hillig, Melt infiltration approach to ceramic matrix composites, J. Am. Ceram. Soc. 71 (2) (1988), https://doi.org/10.1111/j.1151-2916.1988.tb05840.x. C-96–C-99.

[4] R.P. Messner, Y.-M. Chiang, Liquid-phase reaction-bonding of silicon carbide using alloyed silicon-molybdenum melts, J. Am. Ceram. Soc. 73 (5) (1990) 1193–1200, https://doi.org/10.1111/j.1151-2916.1990.tb05179.x.
[5] M. Naikade, C. Hain, K. Kastelik, R. Brönnimann, G. Bianchi, A. Ortona, T. Graule, L. Weber, Liquid Metal Infiltration of Silicon Based Alloys Into Porous Carbonaceous Materials. Part-II: Experimental Verification of Modelling Approaches by Infiltration of Si-Zr Alloy Into Idealised Microchannels, 2021 (unpublished).
[6] M. Naikade, C. Hain, K. Kastelik, A. Parrilli, A. Ortona, T. Graule, L. Weber, Liquid Metal Infiltration of Silicon Based Alloys Into Porous Carbonaceous Materials. Part-III: Experimental Verification of Conversion Products and Infiltration Depth by Infiltration of Si-Zr Alloy Into Carbonaceous And Mixed SiC/Graphite Preforms, 2021 (unpublished).
[7] M. Singh, D.R. Behrendt, Reactive melt infiltration of silicon-molybdenum alloys into microporous carbon preforms, Mater. Sci. Eng. A Struct. Mater. Prop. Microstruct. Process. 194 (2) (1995) 193–200, https://doi.org/10.1016/0921-5093(94)09663-5.
[8] M. Singh, D.R. Behrendt, Reactive melt infiltration of silicon-niobium alloys in microporous carbons, Mater. Res. Soc. 9 (7) (1994) 1701–1708, https://doi.org/10.1557/jmr.1994.1701.
[9] M. Naikade, B. Fankhanel, L. Weber, A. Ortona, M. Stelter, T. Graule, Studying the wettability of Si and eutectic Si-Zr alloy on carbon and silicon carbide by sessile drop experiments, J. Eur. Ceram. Soc. 39 (4) (2019) 735–742, https://doi.org/10.1016/j.jeurceramsoc.2018.11.049.
[10] P.J. Hofbauer, E. Radlein, F. Raether, Fundamental mechanisms with reactive infiltration of silicon melt into carbon capillaries, Adv. Eng. Mater. 21 (8) (2019), https://doi.org/10.1002/adem.201900184.
[11] S. Kumar, A. Kumar, R. Devi, A. Shukla, A.K. Gupta, Capillary infiltration studies of liquids into 3d-stitched C-C preforms. Part b: kinetics of silicon infiltration, J. Eur. Ceram. Soc. 29 (12) (2009) 2651–2657, https://doi.org/10.1016/j.jeurceramsoc.2009.03.006.
[12] E.O. Einset, Capillary infiltration rates into porous media with applications to Silcomp processing, J. Am. Ceram. Soc. 79 (2) (1996) 333–338, https://doi.org/10.1111/j.1151-2916.1996.tb08125.x.
[13] R. Voytovych, R. Israel, N. Calderon, F. Hodaj, N. Eustathopoulos, Reactivity between liquid Si or Si alloys and graphite, J. Eur. Ceram. Soc. 32 (14) (2012) 3825–3835, https://doi.org/10.1016/j.jeurceramsoc.2012.05.020.
[14] O. Dezellus, S. Jacques, F. Hodaj, N. Eustathopoulos, Wetting and infiltration of carbon by liquid silicon, J. Mater. Sci. 40 (9-10) (2005) 2307–2311, https://doi.org/10.1007/s10853-005-1950-7.
[15] A.I. Pommrich, A. Meyer, D. Holland-Moritz, T. Unruh, Nickel self-diffusion in silicon-rich Si-Ni melts, Appl. Phys. Lett. 92 (24) (2008) 241922, https://doi.org/10.1063/1.2947592.
[16] D. Giuranno, A. Polkowska, W. Polkowski, R. Novakovic, Wetting behavior and reactivity of liquid Si-10Zr alloy in contact with glassy carbon, J. Alloys Compds. 822 (2020) 153643, https://doi.org/10.1016/j.jallcom.2020.153643.
[17] J. Qin, X. Li, J. Wang, S. Pan, The self-diffusion coefficients of liquid binary M-Si (M=Al, Fe, Mg and Au) alloy systems by first principles molecular dynamics simulation, AIP Adv. 9 (3) (2019) 035328, https://doi.org/10.1063/1.5067295.